

Similarities and Differences between LaNiO_2 and CaCuO_2 and Implications for Superconductivity

A. S. Botana¹ and M. R. Norman²¹*Department of Physics, Arizona State University, Tempe, Arizona 85287, USA*²*Materials Science and Engineering Division, Argonne National Laboratory, Argonne, Illinois 60439, USA*

(Received 28 August 2019; revised manuscript received 18 November 2019; accepted 23 December 2019; published 4 February 2020)

The recent observation of superconductivity in hole-doped NdNiO_2 has generated considerable attention. The similarities and differences between this infinite-layer nickelates and cuprates are still an open question. To address this issue we derive, via-principles calculations, essential facts related to the electronic structure and magnetism of RNiO_2 ($R = \text{La, Nd}$) in comparison to their cuprate analog CaCuO_2 . From this detailed comparison, we find that RNiO_2 are promising as cuprate analogs. Besides the much larger $d - p$ energy splitting, and the presence of $R 5d$ states near the Fermi energy in the parent compound, all other electronic-structure parameters seem to be favorable in the context of superconductivity as inferred from the cuprates. In particular, the large value of the longer-range hopping t' and the e_g energy splitting are similar to those obtained in cuprates. Doping further acts to increase the cupratelike character of these nickelates by suppressing the self-doping effect of the $R 5d$ bands.

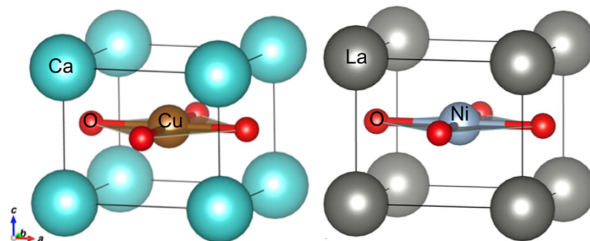
DOI: [10.1103/PhysRevX.10.011024](https://doi.org/10.1103/PhysRevX.10.011024)Subject Areas: Condensed Matter Physics,
Strongly Correlated Materials,
Superconductivity

The quest for finding cuprate analogs in connection with high- T_c superconductivity has followed several routes [1]. Looking at nickelates has been an obvious path: Nickel is next to copper in the periodic table, and if the former could be realized in the $1 +$ oxidation state, it would be isoelectronic with Cu^{2+} [2]. Low-valence-layered nickelates are the closest cuprate analogs in terms of their structure as well as in terms of electron count. This family of materials is represented by the series $\text{R}_{n+1}(\text{NiO}_2)_n\text{O}_2$ ($R = \text{La, Pr, Nd}$, $n = 2, 3, \dots, \infty$). Each member contains n -cupratelike NiO_2 layers. The hard-to-stabilize Ni^{1+} oxidation state is indeed realized in the infinite-layer square planar materials RNiO_2 ($R = \text{La, Nd}$) [3,4] with the same $P4/mmm$ crystal structure as the parent compound of high- T_c cuprates, CaCuO_2 (Fig. 1). The latter has a T_c of 110 K upon hole doping [5]. Still, doubts have been raised that RNiO_2 would be cuprate analogs. Available transport data indicate that LaNiO_2 is not a charge-transfer insulator [6,7] and there is no experimental evidence for antiferromagnetic order in any RNiO_2 material [8]. Electronic-structure calculations

of LaNiO_2 indicate significant differences from CaCuO_2 due to the presence of low-lying $\text{La } 5d$ states, as well as an increased splitting between $\text{Ni } d$ and $\text{O } p$ levels [9–11].

The recent observation of superconductivity in infinite-layer nickelates begs a reconsideration of this earlier thinking. Li *et al.* [12] analyzed thin films of Sr-doped LaNiO_2 with the goal of hole doping the parent phase. However, these samples were not superconducting. In order to emulate the chemical pressure effect already reported for the $n = 3$ member of the series ($\text{La}_4\text{Ni}_3\text{O}_8$ is insulating at low temperature, whereas $\text{Pr}_4\text{Ni}_3\text{O}_8$ is metallic [13]), they turned their attention to the Nd counterpart. Indeed, Sr-doped samples of NdNiO_2 did show a superconducting transition, with an onset at 14.9 K.

In this new context, we analyze the electronic structure of RNiO_2 and do a detailed comparison to that of CaCuO_2 . In order to address the cupratelike character of the 112 nickelates, we focus on three key factors that have been deemed to

FIG. 1. Crystal structure of CaCuO_2 (left) and LaNiO_2 (right).

Published by the American Physical Society under the terms of the [Creative Commons Attribution 4.0 International license](https://creativecommons.org/licenses/by/4.0/). Further distribution of this work must maintain attribution to the author(s) and the published article's title, journal citation, and DOI.

be crucial for superconductivity in cuprates: (1) The charge-transfer energy, $\Delta = \epsilon_d - \epsilon_p$. In cuprates, the smaller Δ , the larger T_c [14]. We find a much larger Δ in $RNiO_2$ with respect to its cuprate analog. (2) The relative strength of longer-range hopping to nearest-neighbor hopping in a one-band model (t'/t ratio). This has been shown by Pavarini *et al.* to correlate with a high T_c in the cuprates [15]. We find an identical t'/t ratio in $RNiO_2$ and $CaCuO_2$. (3) The splitting of the two e_g orbital energies, which also correlates with T_c in cuprates [16]. We find this splitting is also practically identical in the cuprate and nickelate. All in all, our results highlight the importance of the t'/t ratio and the e_g energy splitting for superconductivity, and point to the need to reevaluate the charge-transfer energy criterion as the value of Δ in $RNiO_2$ would put these materials well outside of the bounds for superconductivity in the cuprate context [14].

Computational methods.—Electronic-structure calculations were performed using the all-electron, full-potential code WIEN2k [17] based on the augmented plane wave plus local orbitals (APW + LO) basis set. The Perdew-Burke-Ernzerhof version of the generalized gradient approximation (GGA) [18] was used for the nonmagnetic calculations. The missing correlations beyond GGA at Ni sites were taken into account through LDA + U calculations. Two LDA + U schemes were used: the “fully localized limit” (FLL) and the “around mean field” (AMF) [19,20]. For both schemes, we have studied the evolution of the electronic structure with increasing U ($U_{Ni} = 1.4$ to 6 eV, $J = 0.8$ eV). The lattice parameters used for $LaNiO_2$ were $a = 3.96$ Å, $c = 3.37$ Å, for $NdNiO_2$ $a = 3.92$ Å, $c = 3.28$ Å, for $CaCuO_2$ $a = 3.86$ Å, $c = 3.20$ Å. Supercells of size 2×2 , 3×2 , and 3×3 relative to the primitive $P4/mmm$ cell were employed to study the effect of Sr doping.

To look for possible magnetic solutions, $\sqrt{2} \times \sqrt{2}$ and $\sqrt{2} \times \sqrt{2} \times 2$ cells were constructed. Calculations for different magnetic configurations were performed: (i) ferromagnetic (FM), (ii) antiferromagnetic (AFM) in plane with FM coupling out of plane, (iii) AFM in plane with AFM coupling out of plane. For all calculations, we converged using $R_{mt}K_{max} = 7.0$. The muffin-tin radii used were typical values of 2.5 Å for La and Nd, 2.35 Å for Ca, 2 Å for Ni, 1.95 Å for Cu and 1.72 Å for O. A mesh of $25 \times 25 \times 25$ k points in the irreducible Brillouin zone was used for the nonmagnetic calculations.

To further understand the electronic structure and the comparison of Ni to Cu, we perform an analysis based on maximally localized Wannier functions (MLWFs) [21]. For the spread functional minimization, we used WANNIER90 [22]. Postprocessing of MLWFs to generate tight-binding band structures, hopping integrals, and plots of Wannier orbitals was done with WIEN2WANNIER [23]. These values were also used as start values for a Slater-Koster fit of the electronic structure [24]. In addition, we perform a simple tight-binding fit of the dominant $d_{x^2-y^2}$ - $p\sigma$ antibonding band at the Fermi energy.

Comparison of the nonmagnetic electronic structures of $CaCuO_2$ and $RNiO_2$.—We start by describing some basic aspects of the electronic structure of $CaCuO_2$ and $LaNiO_2$. Figure 1 shows the band structures and orbital-resolved density of states highlighting the Ni/Cu $d_{x^2-y^2}$ and d_{z^2} and O p characters for these two materials. We choose to focus on $LaNiO_2$ rather than its Nd counterpart to avoid issues connected with the R 4*f* states. The effect of La by Nd substitution in the nonmagnetic electronic structure is negligible (Fig. 1 of Ref. [25]; further details contrasting Nd with La can be found here as well).

In both $CaCuO_2$ and $LaNiO_2$, a wide $d_{x^2-y^2}$ band crosses the Fermi level whose bandwidth is reduced by 1 eV in the Ni case with respect to the cuprate due to the increased p - d splitting (see below). The bandwidth of the d_{z^2} band (that appears at lower energies) is in turn increased in the Ni case due to increased hybridization along c .

The most obvious differences between the electronic structures of these two materials arise from the different energies of the spacer cation bands, and the difference in p - d splitting. The Ca 3*d* bands extend down to about 2 eV above the Fermi level, whereas the La 5*d* bands dip down and actually cross the Fermi energy, with the pocket at Γ having mostly La d_{z^2} character, that at A La d_{xy} character. This is consistent with previous work [9–11]. These two electron pockets in the Ni case lead to self-hole-doping of the large holelike $d_{x^2-y^2}$ antibonding Fermi surface (Fig. 2) by about 7%. This self-doping effect from R 5*d* bands is consistent with transport data, which indicates weak localization for $RNiO_2$ [7,12] similar to what is seen in underdoped (as opposed to undoped) cuprates. In addition, this self-doping effect is likely responsible for the suppression of magnetism, and it also implies that the value for optimal doping for T_c could differ from that of the cuprates. The difference in charge-transfer energy between Ni and Cu compounds is obvious from the DOS plot that shows a high degree of p - d hybridization in $CaCuO_2$, whereas in $LaNiO_2$ the O p states are located 3–4 eV below the Ni d bands. More detailed values of on-site energies are given below.

Wannierization.—Since the starting procedure is to assign orbitals localized at specific sites in the initial projection to obtain MLWFs, our choice is to take the obvious set of five Cu/Ni d and six O p orbitals. Inclusion of the La/Ca d_{z^2} orbital improves the fits. The agreement between the band structures obtained from the Wannier function interpolation and that derived from the density-functional theory calculations is excellent, indicating a faithful (though not unique) transformation to MLWFs. The Wannier functions describe d -like orbitals centered on the Ni/Cu sites (with some O p contribution for the $d_{x^2-y^2}$ orbitals) and p -like on the O sites (Fig. 3). The spatial extent of these functions is small and comparable in the Ni and Cu cases (~ 1 Å²).

The on-site energies and hoppings obtained from the Wannier fits are shown in Table I. We note that $\epsilon_d - \epsilon_p$

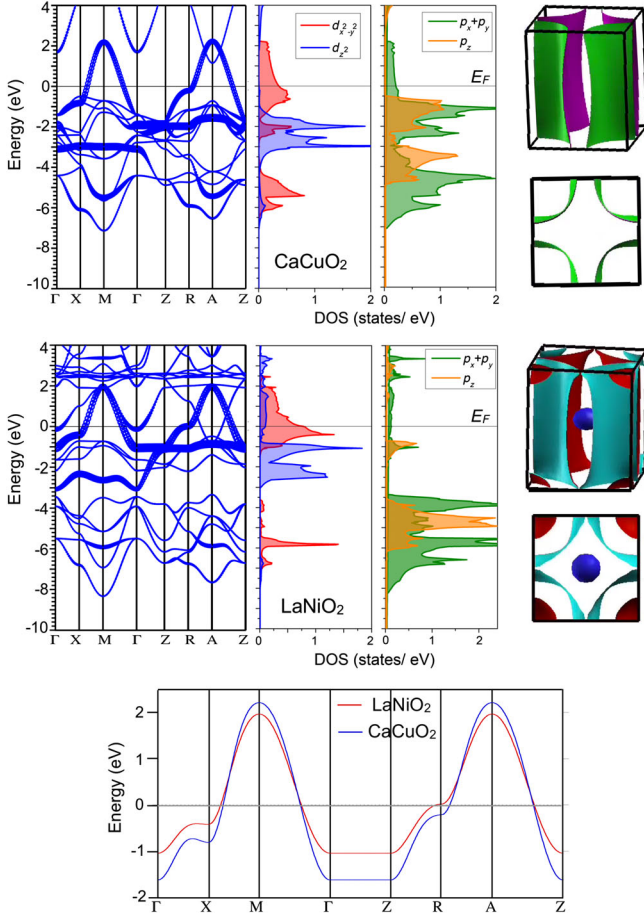


FIG. 2. Top and middle panels. Comparison of the Fermi surface, band structure ($d_{x^2-y^2}$ and d_{z^2} characters highlighted), and orbital-resolved density of states (Ni/Cu $d_{x^2-y^2}$ and d_{z^2} , O p_x , p_y , and p_z) of CaCuO_2 and LaNiO_2 . Bottom panel. Tight binding fit to the $d_{x^2-y^2}$ band at the Fermi energy for both materials.

(referring to $d_{x^2-y^2}$ and $p\sigma$) is 4.4 and 2.7 eV for Ni and Cu, respectively. The former, as mentioned above, is well outside the range observed for cuprates [14]. Remarkably, the pd and pp hopping parameters are almost identical for the two materials, particularly those relevant for the $d_{x^2-y^2}$ and $p\sigma$ orbitals. We in turn have used these parameters as start values for Slater-Koster fits to the band structures as shown in Ref. [25].

Analysis of cuprate criteria in RNiO_2 .—After describing basic aspects of the electronic structure of the parent compounds RNiO_2 and CaCuO_2 , we now turn our attention to the three criteria that have been deemed to correlate with T_c in cuprates: (1) the e_g energy splitting, (2) t'/t ratio, and (3) the charge-transfer energy Δ .

(1) *e_g energy splitting.*—It has been suggested that the T_c of the cuprates is correlated with the splitting of the $d_{x^2-y^2}$ and d_{z^2} energies, with a larger value giving rise to a higher T_c due to reduced mixing of these orbitals [16]. We have compared this energy differ-

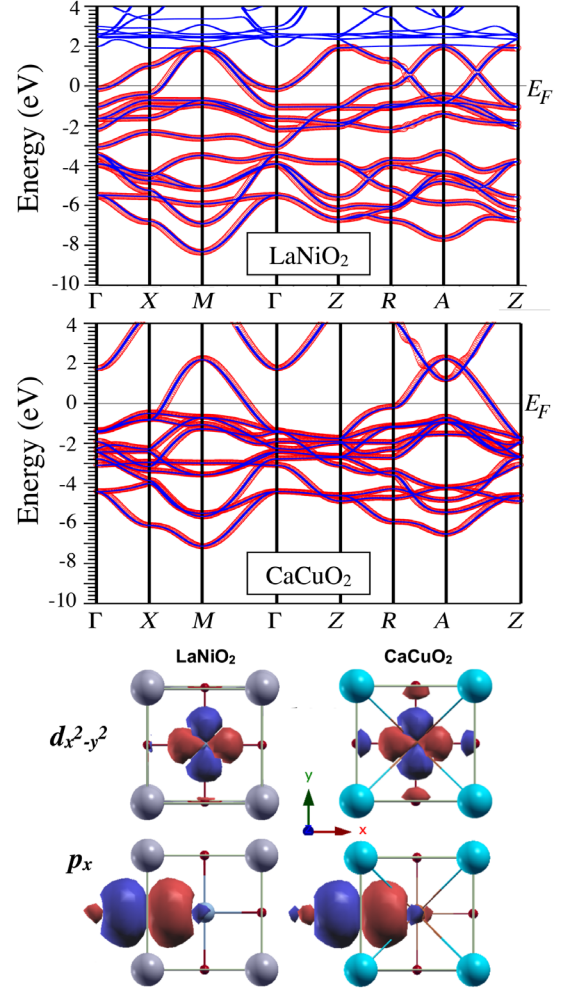


FIG. 3. Wannier fits (red) and density-functional theory band structures (blue) of CaCuO_2 (top) and LaNiO_2 (middle). Comparison of Wannier functions of the $d_{x^2-y^2}$ and p_x character for CaCuO_2 and LaNiO_2 (bottom); the rest are shown in Fig. 2 of Ref. [25]. Colors represent the sign of the Wannier function. The large spheres are the Ca (cyan) and La (gray) atoms.

ence in the Cu and Ni cases using the band centroids calculated as $E_i = \int g_i(E)E dE / \int g_i(E)$, as done in previous work for cuprates [26]. Here, g_i is the partial density of states associated with orbital i . The integration range covers the antibonding band complex for Ni/Cu e_g states. The values we derived for CaCuO_2 are $E_{x^2-y^2} = -0.22$ eV, $E_{z^2} = -2.36$ eV, giving a splitting of 2.14 eV. For LaNiO_2 , $E_{x^2-y^2} = 0.20$ eV, $E_{z^2} = -1.75$ eV, with a comparable splitting of 1.95 eV. From the Wannierization, the splitting between the $d_{x^2-y^2}$ and d_{z^2} energies (0.7 eV for Ni, 1.0 eV for Cu) is considerably smaller than that derived from the integration of the density of states, but still the difference between Ni and Cu is comparable (0.2 eV compared to 0.3 eV).

(2) *t'/t ratio.*—Another quantity that has been deemed important for T_c in the cuprates is the ratio t'/t that

TABLE I. Calculated on-site energies and hoppings for CaCuO₂ and LaNiO₂ derived from the Wannier functions. O1 bonds to Ni/Cu along the x direction, and O2 bonds to Ni/Cu along the y direction.

Wannier on-site energies (eV)	CaCuO ₂	LaNiO ₂
d_{xy}	-2.55	-1.75
$d_{xz,yz}$	-2.44	-1.65
$d_{x^2-y^2}$	-1.51	-1.02
d_{z^2}	-2.48	-1.73
p_x O1	-4.20	-5.41
p_y O1	-2.56	-4.48
p_z O1	-2.72	-4.46
p_x O2	-2.56	-4.47
p_y O2	-4.19	-5.41
p_z O2	-2.72	-4.46
Wannier hoppings (eV)		
$d_{xy} - p_y$ O1	0.71	0.71
$d_{xz} - p_z$ O1	0.75	0.73
$d_{x^2-y^2} - p_x$ O1	-1.20	-1.23
$d_{z^2} - p_x$ O1	0.25	0.20
p_y O2- p_x O1	0.53	0.59
p_x O2- p_x O1	-0.33	-0.27
p_y O2- p_y O1	0.33	0.27
p_x O2- p_y O1	-0.37	-0.16
p_z O2- p_z O1	-0.17	-0.19

describes the relative strength of longer-range hopping to nearest-neighbor hopping in a one-band model—materials with a larger ratio have a higher T_c [15]. To estimate this ratio, we perform a six-parameter tight-binding fit to the $d_{x^2-y^2}$ band at the Fermi energy. Values are listed in Table II along with the associated tight-binding functions, and the resulting band structures are plotted in Fig. 2. Note that these fits differ from those of Lee and Pickett [9]. In particular, we considered longer-range in-plane hoppings, and our interlayer functions also differ, in that they take into account the mixing of

TABLE II. Tight binding fits for the $d_{x^2-y^2}$ band at the Fermi energy for CaCuO₂ and LaNiO₂, along with the ratio t'/t defined as $(|t_3| + |t_2|)/|t_1|$, with $\epsilon(k) = \sum_i t_i f_i(k)$. Here, $\text{wt}(k)$ is $[\cos(k_x a) - \cos(k_y a)]^2/4$. Units are meV. i ranges in the table from 0 to 5, and corresponds to lattice vectors (0,0,0), (1,0,0), (1,1,0), (2,0,0), (0,0,1) and (0,0,2).

f_i	t_i (LaNiO ₂)	t_i (CaCuO ₂)
1	249	201
$2[\cos(k_x a) + \cos(k_y a)]$	-368	-460
$4 \cos(k_x a) \cos(k_y a)$	92	99
$2[\cos(2k_x a) + \cos(2k_y a)]$	-43	-73
$\text{wt}(k) \cos(k_z c)$	-248	-221
$\text{wt}(k) \cos(2k_z c)$	67	50
t'/t	0.37	0.37

relevant “even” (with respect to the diagonal mirror plane) states ($4s$, d_{z^2} , p_z) with the “odd” $d_{x^2-y^2}$ state that has a $[\cos(k_x a) - \cos(k_y a)]^2$ dependence. Then, the t'/t ratio is defined as proposed by Sakakibara *et al.* [16] as $(|t_3| + |t_2|)/|t_1|$. The resulting ratio in both cases is quite large, of order 0.4, comparable to that observed for the highest T_c cuprates. We note, though, that t itself for Ni is 80% of that for Cu due to the increased $d-p$ splitting.

- (3) *Charge-transfer energy.*—Finally, the difference in on-site p and d energies (i.e., the charge-transfer energy) in cuprates has also been correlated with T_c , with smaller values promoting a larger T_c [14]. In this context, the degree of hybridization between the p and d states is reduced in the Ni case with respect to Cu as can be observed from the orbital-resolved density of states (Fig. 2). Moreover, the difference between these two on-site energies found from the Wannier fits for LaNiO₂ well exceeds that seen in the cuprates [14]—a value of 4.4 eV is derived for the nickelate versus 2.7 eV for the cuprate.

Magnetism in RNiO₂.—A C -type AFM state is the ground state of the system from first principles, even at the GGA level, with magnetic moments inside the Ni spheres of $\sim 0.7 \mu_B$. The FM state gives rise to a reduced magnetic moment of $\sim 0.2 \mu_B$ at the GGA level, less stable than the C -type AFM state by 0.72 meV/Ni. The energy difference obtained with respect to the nonmagnetic state is 0.70 and 0.69 meV/Ni with respect to an A -type AFM state. The prediction is then that, although antiferromagnetism should exist in LaNiO₂, the energy gain from the paramagnetic state is small. Additionally, we should note that no experimental evidence for antiferromagnetic order has been reported for RNiO₂. In fact, for LaNiO₂, the susceptibility looks Pauli-like except for a low T upturn that is probably due to nickel metal impurities [4]. As we commented above, the lack of magnetism is likely due to the self-doped holes destroying long-range order, an effect not captured in mean-field simulations.

The results of the LDA + U calculations reported by Anisimov *et al.* [2] for LaNiO₂ gave a stable AFM insulator with the only unoccupied d levels being those of the minority-spin $d_{x^2-y^2}$ orbital. This would then be equivalent to the situation in CaCuO₂. However, we cannot reproduce this insulating state. As U increases, for both the AMF and FLL schemes ($U \geq 4$ eV), hybridization with the La d states causes the Ni d_{z^2} orbitals to rise in energy and stabilizes a metallic AFM ground state even further. This can be clearly observed in Fig. 4 of Ref. [25]. Concomitantly, the value of the magnetic moment at the Ni site increases up to the highest U value used of 6 eV. As stated above, the moments obtained in the FM and AFM states are very different, implying that one cannot map the energies of these states onto a Heisenberg model as done in the cuprates.

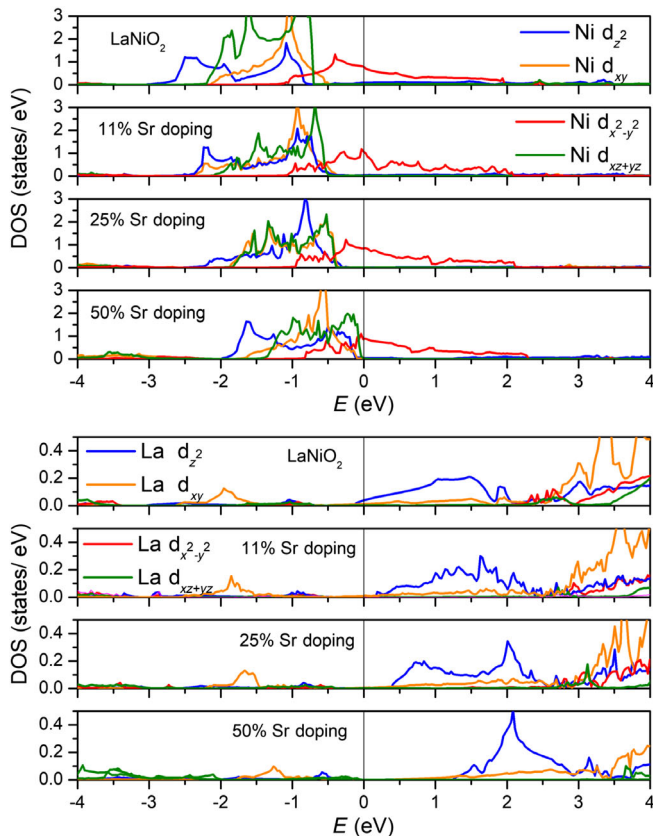


FIG. 4. Comparison of the orbital-resolved Ni d (top panels) and La d (bottom panels) density of states for increasing Sr doping in LaNiO₂.

Doping studies.—As argued above, because of the self-doping from the two R - d electron pockets at Γ and A , the doping for optimal T_c should be different in the nickelate with respect to cuprates. For a more sophisticated analysis of doping, we examine the effect of Sr doping by employing supercells that would give rise to an average d filling of 8.89, 8.75, 8.5, respectively. The corresponding orbital-resolved densities of states for La d and Ni d are shown in Fig. 4. The La d_{xy} character at E_F is diminished upon doping as is the La d_{z^2} character. The concomitant effect can be seen in the orbital-resolved Ni d DOS, where, upon doping, the d_{z^2} DOS above E_F is completely suppressed. This will act to reduce the self-doping effect mentioned above and give a more pure single-band cupratelike picture.

This description of the electronic structure upon doping is consistent with the interpretation of the Hall data for the doped versus undoped material. For the doped case, a low T value of R_H of $+0.4 \times 10^{-3} \text{ cm}^3/\text{C}$ is reported [12]. For this doping (0.2), we obtain, using a rigid band shift of E_F , a value of $+0.2$ which rises to $+0.3$ if the two small La $5d$ pockets are not included (details of the R_H calculation [27] are presented in Ref. [25]). This implies that the large Fermi surface dominates R_H at this doping, consistent with what is found in the cuprates. In contrast, for the undoped

material, values of R_H near zero temperature of -4.6 [7] and $-7.0 \times 10^{-3} \text{ cm}^3/\text{C}$ [6,12] have been reported. This is inconsistent with the presence of a large holelike Fermi surface. Instead, we find a value of -5.2 when restricting the R_H estimate to just the two small La $5d$ electron pockets at Γ and A . This implies that the large holelike Fermi surface is not contributing to the transport in the undoped material, similar to observations for underdoped cuprates.

RNiO₂ materials in the context of other layered nickelates.—RNiO₂ have opened up the possibility of a Ni-based family of unconventional superconductors. In this context, we note that, based on their electronic structure, the $n = 3$ members of the series ($R_4\text{Ni}_3\text{O}_8$) are even more promising as cuprate analogs. With an average Ni valence of 1.33+, these materials are in the overdoped regime of the cuprate phase diagram, and in principle should be superconducting upon electron doping [28]. $R_4\text{Ni}_3\text{O}_8$ compounds have a large orbital polarization, with the involvement of a single band of $d_{x^2-y^2}$ character near the Fermi level (without R $5d$ pockets), and a larger degree of p - d hybridization [13]. In addition, unlike RNiO₂ materials, they offer the possibility of a parent insulating antiferromagnetic phase at d^9 filling [28].

To summarize, despite negative conclusions from earlier work, we find that RNiO₂ are promising as cuprate analogs. To show this, we analyze three key factors for superconductivity in cuprates and compare them to the infinite-layer nickelate. In particular, we find an identical t'/t ratio and near identical e_g splitting in RNiO₂ and CaCuO₂. The main difference between the two materials is the charge-transfer energy $\Delta = \epsilon_d - \epsilon_p$, much larger in RNiO₂. Our results point to the need to reexamine this last criterion for superconductivity as the derived Δ puts the nickelates well outside the bounds for superconductivity in the cuprate context (though it could be responsible for the suppressed value of T_c). Another difference in the parent RNiO₂ compounds is the presence of R $5d$ states near the Fermi energy in the parent phase. However, we emphasize that Sr doping further acts to increase the cupratelike character by suppressing this self-doping effect. In retrospect, then, the discovery of superconductivity in Sr-doped NdNiO₂ should not be as surprising as it has turned out to be. In that context, we should note that electron doping of SrCuO₂ leads to the highest T_c among electron-doped cuprates [29]. Therefore, electron doping of NdNiO₂ could be equally revealing. Finally, other members of the square-planar layered nickelate family should be equally promising candidates for high- T_c superconductivity.

ACKNOWLEDGMENTS

The authors would like to thank John Mitchell for discussions. This work was supported by the Materials Sciences and Engineering Division, Basic Energy Sciences, Office of Science, U.S. Department of Energy. A. S. B. thanks ASU for startup funds, and also ANL for hosting her

visit where this project was initiated. We acknowledge the computing resources provided on Blues, a high-performance computing clusters operated by the Laboratory Computing Resource Center at Argonne National Laboratory. A. S. B. acknowledges the Research Computing Center at ASU for HPC resources.

-
- [1] M. R. Norman, *Materials Design for New Superconductors*, *Rep. Prog. Phys.* **79**, 074502 (2016).
- [2] V. I. Anisimov, D. Bukhvalov, and T. M. Rice, *Electronic Structure of Possible Nickelate Analogs to the Cuprates*, *Phys. Rev. B* **59**, 7901 (1999).
- [3] M. Crespin, P. Levitz, and L. Gatinéau, *Reduced Forms of LaNiO₃ Perovskite. Part 1. Evidence for New Phases: La₂Ni₂O₅ and LaNiO₂*, *J. Chem. Soc., Faraday Trans. 2* **79**, 1181 (1983).
- [4] M. A. Hayward, M. A. Green, M. J. Rosseinsky, and J. Sloan, *Sodium Hydride as a Powerful Reducing Agent for Topotactic Oxide Deintercalation: Synthesis and Characterization of the Nickel(I) Oxide LaNiO₂*, *J. Am. Chem. Soc.* **121**, 8843 (1999).
- [5] M. Azuma, Z. Hiroi, M. Takano, Y. Bando, and Y. Takeda, *Superconductivity at 110 K in the Infinite-Layer Compound (Sr_{1-x}Ca_x)_{1-y}CuO₂*, *Nature (London)* **356**, 775 (1992).
- [6] A. Ikeda, T. Manabe, and M. Naito, *Improved Conductivity of Infinite-Layer LaNiO₂ Thin Films by Metal Organic Decomposition*, *Physica (Amsterdam)* **495C**, 134 (2013).
- [7] A. Ikeda, Y. Krockenberger, H. Irie, M. Naito, and H. Yamamoto, *Direct Observation of Infinite NiO₂ Planes in LaNiO₂ Films*, *Appl. Phys. Express* **9**, 061101 (2016).
- [8] M. A. Hayward and M. J. Rosseinsky, *Synthesis of the Infinite Layer Ni(I) Phase NdNiO_{2+x} by Low Temperature Reduction of NdNiO₃ with Sodium Hydride*, *Solid State Sci.* **5**, 839 (2003).
- [9] K.-W. Lee and W. E. Pickett, *Infinite-Layer LaNiO₂: Ni¹⁺ Is Not Cu²⁺*, *Phys. Rev. B* **70**, 165109 (2004).
- [10] T. Liu, H. Wu, T. Jia, X. Zhang, Z. Zeng, H. Q. Lin, and X. G. Li, *Dimensionality-Induced Insulator-Metal Crossover in Layered Nickelates La_{n+1}Ni_nO_{2n+2} (n = 2, 3, and ∞)*, *AIP Adv.* **4**, 047132 (2014).
- [11] A. S. Botana and M. R. Norman, *Layered Palladates and Their Relation to Nickelates and Cuprates*, *Phys. Rev. Mater.* **2**, 104803 (2018).
- [12] D. Li, K. Lee, B. Y. Wang, M. Osada, S. Crossley, H. R. Lee, Y. Cui, Y. Hikita, and H. Y. Hwang, *Superconductivity in an Infinite-Layer Nickelate*, *Nature (London)* **572**, 624 (2019).
- [13] J. Zhang, A. S. Botana, J. W. Freeland, D. Phelan, Hong Zheng, V. Pardo, M. R. Norman, and J. F. Mitchell, *Large Orbital Polarization in a Metallic Square-Planar Nickelate*, *Nat. Phys.* **13**, 864 (2017).
- [14] C. Weber, C. Yee, K. Haule, and G. Kotliar, *Scaling of the Transition Temperature of Hole-Doped Cuprate Superconductors with the Charge-Transfer Energy*, *Europhys. Lett.* **100**, 37001 (2012).
- [15] E. Pavarini, I. Dasgupta, T. Saha-Dasgupta, O. Jepsen, and O. K. Andersen, *Band-Structure Trend in Hole-Doped Cuprates and Correlation with T_{c,max}*, *Phys. Rev. Lett.* **87**, 047003 (2001).
- [16] H. Sakakibara, H. Usui, K. Kuroki, R. Arita, and H. Aoki, *Origin of the Material Dependence of T_c in the Single-Layered Cuprates*, *Phys. Rev. B* **85**, 064501 (2012).
- [17] P. Blaha, K. Schwarz, G. K. H. Madsen, D. Kvasnicka, and J. Luitz, *An Augmented Plane Wave Plus Local Orbitals Program for Calculating Crystal Properties* (Vienna University of Technology, Austria, 2001).
- [18] J. P. Perdew, K. Burke, and M. Ernzerhof, *Generalized Gradient Approximation Made Simple*, *Phys. Rev. Lett.* **77**, 3865 (1996).
- [19] A. I. Liechtenstein, V. I. Anisimov, and J. Zaanen, *Density-Functional Theory and Strong Interactions: Orbital Ordering in Mott-Hubbard Insulators*, *Phys. Rev. B* **52**, R5467 (1995).
- [20] M. T. Czyżyk and G. A. Sawatzky, *Local-Density Functional and On-Site Correlations: The Electronic Structure of La₂CuO₄ and LaCuO₃*, *Phys. Rev. B* **49**, 14211 (1994).
- [21] N. Marzari, A. A. Mostofi, J. R. Yates, I. Souza, and D. Vanderbilt, *Maximally Localized Wannier Functions: Theory and Applications*, *Rev. Mod. Phys.* **84**, 1419 (2012).
- [22] A. A. Mostofi, J. R. Yates, G. Pizzi, Y.-S. Lee, I. Souza, D. Vanderbilt, and N. Marzari, *An Updated Version of WANNIER90: A Tool for Obtaining Maximally-Localised Wannier Functions*, *Comput. Phys. Commun.* **185**, 2309 (2014).
- [23] J. Kunes, R. Arita, P. Wissgott, A. Toschi, H. Ikeda, and K. Held, *Wien2wannier: From Linearized Augmented Plane Waves to Maximally Localized Wannier Functions*, *Comput. Phys. Commun.* **181**, 1888 (2010).
- [24] J. C. Slater and G. F. Koster, *Simplified LCAO Method for the Periodic Potential Problem*, *Phys. Rev.* **94**, 1498 (1954).
- [25] See Supplemental Material at <http://link.aps.org/supplemental/10.1103/PhysRevX.10.011024> for further details of the band structures, Wannier functions, Slater-Koster fits, and magnetic band structures.
- [26] S. W. Jang, T. Kotani, H. Kino, K. Kuroki, and M. J. Han, *Quasiparticle Self-Consistent GW Study of Cuprates: Electronic Structure, Model Parameters and the Two-Band Theory for T_c*, *Sci. Rep.* **5**, 12050 (2015).
- [27] M. R. Norman, *Hall Number in YbRh₂Si₂*, *Phys. Rev. B* **71**, 220405(R) (2005).
- [28] A. S. Botana, V. Pardo, and M. R. Norman, *Electron Doped Layered Nickelates: Spanning the Phase Diagram of the Cuprates*, *Phys. Rev. Mater.* **1**, 021801 (2017).
- [29] M. G. Smith, A. Manthiram, J. Zhou, J. B. Goodenough, and J. T. Markert, *Electron-Doped Superconductivity at 40 K in the Infinite-Layer Compound Sr_{1-y}Nd_yCuO₂*, *Nature (London)* **351**, 549 (1991).